A Density Functional Theory (DFT) Study on the Effect of Chlorine in the Magnesium Zinc Oxide (MZO) Front Interface for Cadmium Telluride (CdTe) Thin Film Solar Cells

Aanand Thiyagarajan
Department of Mechanical Engineering
Colorado State University
Fort Collins, USA
athiyag@colostate.edu

Anthony Nicholson
Department of Mechanical Engineering
Colorado State University
Fort Collins, USA
apnichol@rams.colostate.edu

Akash Shah
Department of Mechanical Engineering
Colorado State University
Fort Collins, USA
ashah54@colostate.edu

Walajabad Sampath
Department of Mechanical Engineering
Colorado State University
Fort Collins, USA
sampath@colostate.edu

***Abstract*—Cadmium telluride photovoltaics has benefitted greatly from the cadmium chloride treatment which causes a remarkable improvement in cell efficiencies. This work investigates the effect of elemental chlorine at the interface between the magnesium zinc oxide front contact and the cadmium telluride absorber in such a device. Band alignment including band bending and interface states and its role in potential charge carrier transport is the key feature studied. It is seen that a small amount of chlorine is leads to a more desirable band alignment. Higher concentrations of chlorine result in unfavorable band characteristics.**

Keywords—chlorine, atomistic, thin film, interface, oxide, photovoltaic, band alignment, DFT, NEGF

I. Introduction

Cadmium telluride (CdTe) has established itself as a prominent thin film photovoltaic technology over the last decade. The fabrication process for such devices has been streamlined over the years to reach the small scale and module efficiencies as they stand today. Devices fabricated at the Next Generation Photovoltaic (NGPV) center at Colorado State University have employed a CdTe absorber layer with current efforts moving to a graded cadmium selenium telluride (CdSeTe or CST) replacing the CdTe [1,2]. Magnesium Zinc Oxide (MgZnO or MZO) links the CdTe absorber to the Transparent Conducting Oxide (TCO) at the front [3]. A magnesium atomic concentration of 23% in the MZO alloy has furnished the best cells [1].

An important step in the procedure is the cadmium chloride ($CdCl_2$) annealing treatment that transforms the device dramatically. This can result in cells with power conversion efficiencies close to 20% as opposed to almost no power output without the treatment [4]. Many theories have been put forward that attribute the effectiveness of the $CdCl_2$ treatment process. Some of them include lowering point defect concentrations, passivation of recombination centers, stacking fault correction, formation of n-type regions that facilitate electron-hole separation and reduction of mid-gap states while maintaining charge separation [5].

Chen Li et al have observed an enrichment of chlorine (Cl) in CdTe grain boundaries, with atomic concentrations between 20 and 30% [4]. At these locations, there is a corresponding decrease in the concentration of elemental tellurium (Te), suggesting that the chlorine occupies the Te sites preferentially. NanoSIMS (Secondary Ion Mass Spectroscopy) measurements have revealed the presence of chlorine at the front interface between MZO and CdTe, although the concentration is unknown.

This research aims to examine the effect of $CdCl_2$ from an atomic scale perspective using first-principles modeling based on Density Functional Theory (DFT) [6]. The technique is used along with the Non-Equilibrium Green's Function (NEGF) formalism and other semi-empirical methods [7]. Such a study for oxide interfaces in CdTe has not been carried out before.

II. Methods

The atomistic simulations were carried out with the help of the Synopsys QuantumATK version Q-2019.12 DFT LCAO (Linear Combination of Atomic Orbitals) calculator [8-10]. The GGA (Generalized Gradient Approximation) exchange correlation (XC) in combination with the PBE (Perdew-Burke-Ernzerhof) functional and SG15 pseudopotentials were used throughout [11,12]. MZO was created by substituting 23% of the zinc atoms randomly in the zinc oxide (ZnO) lattice. It has been reported that the MZO alloy maintains the wurtzite structure of its parent binary compound ZnO up to a Mg concentration of 46% [13]. The MZO-CdTe interface model was created using the interface builder in NanoLab [14]. The MZO and CdTe were cleaved along the (0002) and (111) planes respectively as they were the most preferred crystallographic plane orientations of the as-deposited materials [15]. Moreover, it has been observed that (111) plane orientation is maintained even after the $CdCl_2$ treatment [1]. Two interface terminations were explored – magnesium/zinc-tellurium (Mg/Zn-Te) and

Identify applicable funding agency here. If none, delete this text box.

oxygen-cadmium (O-Cd) – in accordance with previous studies [16]. The former was a straightforward construction using the builder tool with MZO as the left interface and CdTe as the right counterpart. The assembly of an O-Cd terminated interface started with assigning CdTe as the left interface and MZO as the right. This structure was then rotated by 180 degrees about the axis perpendicular to both interface plane and the device along its length. An interface strain of 4% between the surfaces was chosen as the model size was unwieldy at lower strains. Right at the interface, the Te atoms were substituted with Cl at varying percentages from 0% through 100% at intervals of 25%. The interface was subject to geometry optimization (GO) where the atoms were structurally relaxed to a force threshold of 0.05 eV/Å. Only the first unit cell of the interface was relaxed. This amounted to a relaxation length of 15 nm. The rest of the atoms on the MZO side of the supercell were fixed in place while the corresponding atoms on the CdTe side were confined to a rigid constraint for them to move along with the relaxed atoms. A two-probe setup was used to generate a device configuration from the relaxed interface [17]. After an electronic structure or self-consistent field (SCF) calculation, analyses were performed on the resulting file. This consisted of a projected local density of states (PLDOS) calculation for the length of the device. The interface calculations employed a Monkhorst-Pack grid of 4x4 k-points while a 4x4x182 mesh was opted for the device simulations [18]. Density Mesh Cutoff values of 2200 eV and 3700 eV were used for CdTe and MZO respectively [19]. The DFT-1/2 semi-empirical method was used to improve upon band gaps that are frequently underestimated by standard DFT [20]. In combination with the GGA XC functional, this method is also referred to as GGA-1/2 [21].

III. Results And Discussion

TABLE I. Bulk Properties Of CdTe

Parameter	Method					
	LDA	*LDA -1/2*	*GGA*	*GGA -1/2*	*Experiment*	*Error %*
Lattice constant (A)	6.55	-	6.66	-	6.48	2.7
Band gap (eV)	0.84	1.63	0.77	1.47	1.49	1.3

TABLE II. Bulk Properties Of MZO

Parameter	Method					
	LDA	*LDA -1/2*	*GGA*	*GGA -1/2*	*Experiment*	*Error %*
Lattice constant (A)	a=5.29 c=3.27	-	a=5.28 c=3.30	-	a=5.18 c=3.25	1.5 1.5
Band gap (eV)	0.67	2.88	0.65	3.56	3.70	4

Bulk lattice constants and band gaps shown in tables I and II matched well with those reported in the literature [13, 22, 23]. The interface structure after GO did not show any unusual rearrangement of atoms. An illustration of the interface before and after GO in Fig. 1 and Fig. 2 below show that the atoms have moved a small amount. The displacement of atoms on the MZO side is very minimal but the Cd and Te atoms have moved enough such that they are not directly behind the atoms in the front plane.

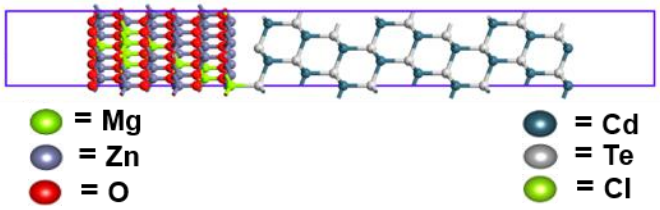

Fig. 1. MZO-CdTe interface before geometry optimization

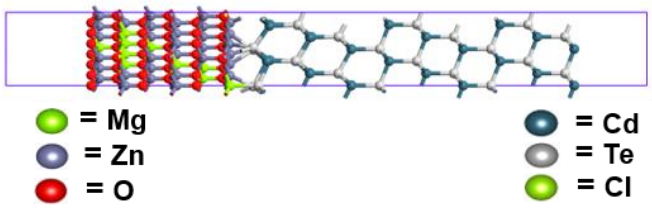

Fig. 2. MZO-CdTe interface after geometry optimization

Band alignment is the primary feature of interest and the band gap values and band offsets at different points along the length of the device have been tabulated below. The band gap (E_g) of both the interface materials have not converged to their bulk values, possibly due to the somewhat short device length of ~225 Å. Exceeding this length would require more computational resources than those currently available to the authors. However, since the primary interest was in observing band alignment at the interface, this length was deemed enough.

TABLE III. Band Gaps and Band Offests For The MZO-CdTe Interface

Band alignment comparison	Values (eV)		
	MZO bulk E_g	*Band offset*	*CdTe bulk E_g*
O-Cd terminated, No Cl	2.81	1.23	1.70
O-Cd terminated, 25% Cl_{Te}	2.81	1.21	1.67
O-Cd terminated, 50% Cl_{Te}	2.82	1.81	1.73
O-Cd terminated, 75% Cl_{Te}	2.90	1.96	1.74
O-Cd terminated, 100% Cl_{Te}	3.05	1.88	1.73
Mg/Zn-Te terminated, No Cl	3.48	-1.53	1.98
Mg/Zn-Te terminated, 25% Cl_{Te}	3.45	-1.62	2.00

In the case of the O-Cd terminated models, bulk band gap values for MZO gradually rise from 2.81 eV with no Cl to 3.05 eV when all Te atoms are replaced with Cl. The band gap of CdTe remains steady throughout. The CBO generally follows an increasing trend going to 0% to 100% Cl. The interface looks clean at low Cl concentrations (0%, 25% and 50%) but states do appear at higher amounts (75% and 100%). Another interesting feature is the gradual downward bending of both conduction and valence bands of CdTe as the Cl concentration goes up. This

results in the band gap at the interface decreasing with increasing amounts of Cl.

For Mg/Zn-Te terminated MZO-CdTe, the VB offset (indicated by a negative sign) is 1.53 eV without Cl. The bulk band gaps are 3.48 eV for MZO and 1.98 eV for CdTe with some interface states present. On substitution of 25% interface Te sites with Cl, these respective values are 3.45 eV and 2.0 eV. The VB offset is 1.62 eV. The interface states do not disappear; however, states close to the CB are alleviated while more states are formed close to the Fermi level.

The above values were obtained from PLDOS images of the device shown below. The pink regions indicate the existence of a high density of states; the blue areas show a lower number of possible states and the territory covered in black equates to forbidden energy values.

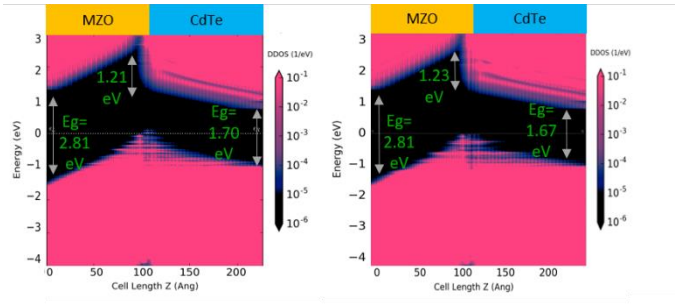

Fig. 3. PLDOS plots for O-Cd terminated MZO-CdTe a) without Cl b) with 25% Cl_{Te}.

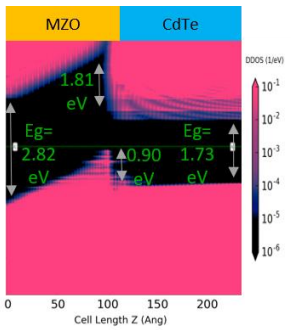

Fig. 4. PLDOS plots for O-Cd terminated MZO-CdTe with 50% Cl_{Te}.

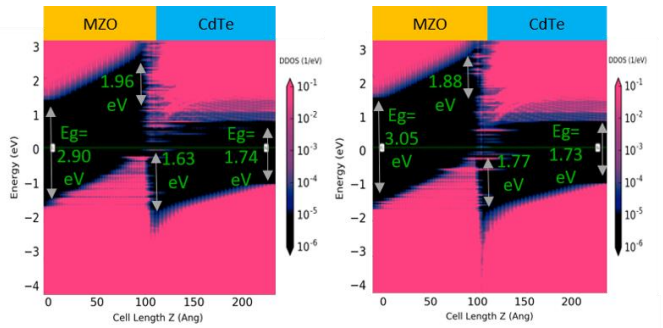

Fig. 5. PLDOS plots for O-Cd terminated MZO-CdTe with a)75% Cl_{Te} b) 100% Cl_{Te}.

Shown above are PLDOS plots for O-Cd terminated Comparing the different images, Cl concentrations of 0% and 25% lead to clean band gaps. The latter seems to have a higher Eg value at the interface as the states around the Fermi level have been erased. This suggests that Cl up to a concentration of 25% passivates the interface by removing states close to the valence and conduction bands. As the number of Cl atoms at the interface increases, thereby increasing the ratio, the effect is more detrimental as several interface states begin to form.

The above figures indicate that the band alignment may not favor electron transport through the MZO to the front of the device. This is due to a very high CBO (>1 eV). Electrons assisted by thermionic emission may possess enough energy to cross a lower barrier (<0.4 eV) at room temperature [24]. Movement of holes will also be restricted due to the VB on the CdTe side bending down away from the interface.

In the case of Mg/Zn-Te terminations, only 0% and 25% Cl have been simulated. Convergence has not yet been reached for calculations involving higher amounts of Cl. Efforts are currently being undertaken to achieve this. This trend has been observed in the O-Cd termination case and is expected to follow a similar trend with the Mg/Zn-Te terminated models. A narrowing of the band gap can also be observed. Moreover, a dip in the valence band on the CdTe side is noticed as the amount of Cl goes up. Cl at a concentration of 25% provides the best band alignment. This may indicate that Cl concentrations at the MZO-CdTe interface resemble those at the grain boundaries as determined by the experimental findings of Li et al.

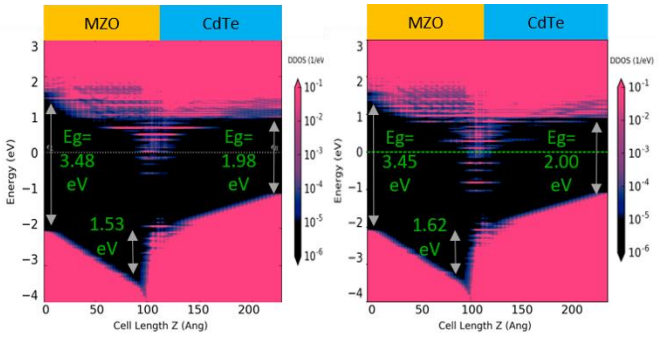

Fig. 6. PLDOS plots for Mg/Zn-Te terminated MZO-CdTe a) without Cl b) with 25% Cl_{Te}.

For the Mg/Zn-Te terminations, the band alignment generates a barrier in the VB which can help in retaining the holes within the CdTe and shunting them to the back of the device. The electron barrier, although present is not as high as the one found in the O-Cd termination case,

It is also noted that these simulations were performed for intrinsic materials. Ways to overcome this problem and "flatten" the bands is by incorporating doping in the device to levels that have been seen experimentally or by applying a voltage bias. In general, the higher the doping, the faster the bands converge to their bulk material values with respect to distance from the interface. These steps, along with the mechanism involved in the chlorine passivation of the MZO-CdTe interface are in progress and will be presented in subsequent works.

IV. Conclusion And Future Work

Atomistic modeling in combination with NEGF and semi empirical methods were used to obtain a band alignment perspective of the effect of chlorine on MZO-CdTe interfaces. The DFT calculations provide a lot of detail regarding band gaps, bending and interface states which may not be observed using one dimensional modeling techniques.

Perhaps the most striking feature is the dependence of band alignment on the interface termination. In general, the O-Cd termination bends both the CB and VB upwards, while a Mg/Zn-Te termination does the opposite and bends both bands down. This is the case for models without Cl or small amounts of Cl. This may have practical implications for device fabrication where deposition can be controlled to an atomic level. Processes can then be tuned to arrive at the desired interface termination.

25% Cl is seen to improve band alignment characteristics at the interface by alleviating states close to the valence and conduction bands. Higher doses of chlorine though may have a negative impact by lowering the band gap and increasing the density of interface states. Thus, DFT simulations provide nuances not captured by other methods while also matching experimental findings.

Perkins et al discovered the presence of a complex CdTe native oxide and an atomically thin layer of $CdCl_2$ at the interface between Al_2O_3 and CdTe [25]. However, modeling such a configuration was considered out of scope of this work. More expertise is required in modeling interfaces with three materials and further detail needs to be known about the native CdTe oxide that is formed. Higher Cl concentrations will be tested with the Mg/Zn-Te terminated interface, as will models including doping and voltage bias.

Acknowledgment

This work was performed through the aid of the National Science Foundation (NSF) INTERN (award ID 1538733) and the Industry University Cooperative Research Center (I/UCRC) programs. The authors would like to thank Dr. Umberto Martinez Pozzoni and Synopsys Denmark for providing technical guidance during the course of the project. This research utilized the Summit supercomputer, which is supported by the National Science Foundation (awards ACI-1532235 and ACI-1532236), the University of Colorado Boulder and Colorado State University.

References

[1] Amit H.Munshi, Jason M.Kephart, AliAbbas, Tushar M.Shimpi, Kurt L.Barth, John M.Walls, Walajabad S.Sampath, Polycrystalline CdTe photovoltaics with efficiency over 18% through improved absorber passivation and current collection, Solar Energy Materials and Solar Cells Volume 176 March 2018, Pages 9-18.

[2] Fiducia, T.A.M., Mendis, B.G., Li, K. et al. Understanding the role of selenium in defect passivation for highly efficient selenium-alloyed cadmium telluride solar cells. Nat Energy 4, 504–511 (2019).

[3] J.M.Kephart, J.W.McCamy, Z.Ma, A.Ganjoo F.M.Alamgir, W.S.Sampath, Band alignment of front contact layers for high-efficiency CdTe solar cells Solar Energy Materials and Solar Cells, Volume 157, December 2016, Pages 266-275.

[4] Li et al, Grain-Boundary-Enhanced Carrier Collection in CdTe Solar Cells, PhysRevLett 2014.

[5] I. M. Dharmadasa, Review of the CdCl2 Treatment Used in CdS/CdTe Thin Film Solar Cell Development and New Evidence towards Improved Understanding, Coatings 2014, 4, 282-307.

[6] W. Kohn and L.J. Sham, Self-Consistent Equations Including Exchange and Correlation Effects Phys. Rev. 140, A1133-A1138 (1965).

[7] M. Brandbyge, J. L. Mozos, P. Ordejón, J. Taylor, and K. Stokbro, Density-functional method for nonequilibrium electron transport, Phys. Rev. B 65, 165401 (2002).

[8] S. Smidstrup et al., "QuantumATK: An integrated platform of electronic and atomic-scale modelling tools", J. Phys.: Condens. Matter 32, 015901 (2020).

[9] S. Smidstrup, D. Stradi, J. Wellendorff, P. A. Khomyakov, U. G. Vej-Hansen, M-E. Lee, T. Ghosh, E. Jónsson, H. Jónsson, and K. Stokbro, First-principles Green's-function method for surface calculations: A pseudopotential localized basis set approach, Phys. Rev. B 96, 195309 (2017).

[10] Robert S. Mulliken's Nobel Lecture, Science, 157, no. 3784, 13 - 24, (1967).

[11] J. P. Perdew, K. Burke, and M. Ernzerhof, Generalized Gradient Approximation Made Simple, Phys. Rev. Lett. 77, 3865 (1996).

[12] M. Schlipf and F. Gygi, Optimization algorithm for the generation of ONCV pseudopotentials, Comp. Phys. Comm. 196, 36 (2015).

[13] Takashi Minemoto, Takayuki Negami, Shiro Nishiwaki, Hideyuki Takakura, Yoshihiro Hamakawa, Preparation of Zn1-xMgxO films by radio frequency magnetron sputtering, Thin Solid Films 372 _2000. 173-176.

[14] D. Stradi, L. Jelver, S. Smidstrup and K. Stokbro, Method for determining optimal supercell representation of interfaces, IOP Publishing, J. Phys.: Condens. Matter 29, 185901 (7pp) (2017).

[15] T. Ablekim *et al.*, "Tailoring MgZnO/CdSeTe Interfaces for Photovoltaics," in *IEEE Journal of Photovoltaics*, vol. 9, no. 3, pp. 888-892, May 2019.

[16] John E. Jaffe, Tiffany C. Kaspar, Timothy C. Droubay, and Tamas Varga, Band offsets for mismatched interfaces: The special case of ZnO on CdTe (001), Journal of Vacuum Science & Technology A 31, 061102 (2013).

[17] D. Stradi, U. Martinez, A. Blom, M. Brandbyge, K. Stokbro, General atomistic approach for modeling metal-semiconductor interfaces using density functional theory and nonequilibrium Green's function, Phys. Rev. B 93, 155302 (2016).

[18] H. J. Monkhorst and J. D. Pack, Special points for Brillouin-zone integrations, Phys. Rev. B 13, 5188 (1976).

[19] Jeffrey R. Reimers, Computational Methods for Large Systems: Electronic Structure Approaches for Biotechnology and Nanotechnology, ISBN: 978-0-470-93472-2 (2011).

[20] Jason M. Crowley, Jamil Tahir-Kheli, and William A. Goddard, Resolution of the Band Gap Prediction Problem for Materials Design, The Journal of Physical Chemistry Letters, 2016.

[21] Luiz G. Ferreira, Marcelo Marques, and Lara K. Teles. Slater half-occupation technique revisited: the LDA-1/2 and GGA-1/2 approaches for atomic ionization energies and band gaps in semiconductors. AIP Adv., 1(3):032119, 2011.

[22] Sanjeev Kumar et al, Structural and optical properties of magnetron sputtered MgxZn1−xO thin films 2006 J. Phys.: Condens. Matter 18 3343.

[23] A. Suryanarayana Reddy, P. Prathap, Y.P.V. Subbaiah, K.T. Ramakrishna Reddy, J. Yi Growth and physical behaviour of Zn1−xMgxO films, Thin Solid Films 516 (2008).

[24] Daisuke Hironiwa, Nobuki Matsuo, Noriyuki Sakai, Takuya Katou, Hiroki Sugimoto, Jakapan Chantana, Zeguo Tang and Takashi Minemoto, Sputtered (Zn,Mg)O buffer layer for band offset control in Cu2ZnSn(S,Se)4 solar cells, The Japan Society of Applied Physics 2014.

[25] Perkins, Craig et al, (2018) Interfaces Between CdTe and ALD Al2O3. IEEE Journal of Photovoltaics. PP. 1-4.